



# Influence of $^{235}\text{U}$ enrichment on the moderator temperature coefficient of reactivity in a graphite-moderated molten salt reactor

Xiao-Xiao Li<sup>1,2</sup> · De-Yang Cui<sup>1,2</sup> · Yu-Wen Ma<sup>1,2</sup> · Xiang-Zhou Cai<sup>1,2,3</sup> · Jin-Gen Chen<sup>1,2,3</sup>

Received: 28 February 2019 / Revised: 11 July 2019 / Accepted: 13 July 2019 / Published online: 23 October 2019  
 © China Science Publishing & Media Ltd. (Science Press), Shanghai Institute of Applied Physics, the Chinese Academy of Sciences, Chinese Nuclear Society and Springer Nature Singapore Pte Ltd. 2019

**Abstract** To optimize the temperature coefficient of reactivity (TCR) for a graphite-moderated and liquid-fueled molten salt reactor, the effects of fuel salt composition on the fuel salt temperature coefficient of reactivity (FSTC) were investigated in our earlier work. In this study, we aim to provide a more comprehensive analysis of the TCR by considering the effects of the graphite-moderator temperature coefficient of reactivity (MTC). The effects of  $^{235}\text{U}$  enrichment and heavy metal (HM) proportion in the salt mixture on the MTC are investigated from the perspective of the six-factor formula based on a full-core model. For the MTC (labeled “ $\alpha_{\text{TM}}$ ”), the temperature coefficient of the fast fission factors ( $\alpha_{\text{TM}}(\varepsilon)$ ) is positive, while those of the resonance escape probability ( $\alpha_{\text{TM}}(p)$ ), the thermal reproduction factor ( $\alpha_{\text{TM}}(\eta)$ ), the thermal utilization factor ( $\alpha_{\text{TM}}(f)$ ), and the total non-leakage probability ( $\alpha_{\text{TM}}(\Lambda)$ )

are negative. The results reveal that the magnitudes of  $\alpha_{\text{TM}}(\varepsilon)$  and  $\alpha_{\text{TM}}(p)$  for the MTC are similar. Thus, variations in the MTC with  $^{235}\text{U}$  enrichment for different HM proportions are mainly dependent on  $\alpha_{\text{TM}}(\eta)$ ,  $\alpha_{\text{TM}}(\Lambda)$ , and  $\alpha_{\text{TM}}(f)$ , but especially on the former two. To obtain a more negative MTC, a lower HM proportion and/or a lower  $^{235}\text{U}$  enrichment is recommended. Together with our previous studies on the FSTC, a relatively soft neutron spectrum could strengthen the TCR with a sufficiently negative MTC.

**Keywords** Molten salt reactor (MSR) · Moderator temperature coefficient of reactivity (MTC) · Six-factor formula

## List of symbols

|                                   |   |
|-----------------------------------|---|
| TCR                               | Temperature coefficient of reactivity                     |
| FSTC                              | Fuel salt temperature coefficient of reactivity           |
| MTC                               | Moderator temperature coefficient of reactivity           |
| HM                                | Heavy metal   |
| $\varepsilon$                     | Fast fission factor                                       |
| $p$                               | Resonance escape probability                              |
| $\eta$                            | Thermal reproduction factor                               |
| $f$                               | Thermal utilization factor                                |
| $\Lambda$                         | Total non-leakage probability                             |
| $\alpha_{\text{TM}}$              | Symbol for MTC  |
| $\alpha_{\text{TM}}(\varepsilon)$ | Temperature coefficient for $\varepsilon$                 |
| $\alpha_{\text{TM}}(\eta)$        | Temperature coefficient for $\eta$                        |
| $\alpha_{\text{TM}}(\Lambda)$     | Temperature coefficient for $\Lambda$                     |
| $\alpha_{\text{TM}}(p)$           | Temperature coefficient for $p$                           |
| $\alpha_{\text{TM}}(f)$           | Temperature coefficient for $f$                           |
| EALF                              | Energy of average lethargy of fission                     |
| Fiss                              | Thermal production: neutron production by thermal fission |

This work was supported by the Chinese TMSR Strategic Pioneer Science and Technology Project (No. XDA02010000) and the Frontier Science Key Program of the Chinese Academy of Sciences (No. QYZDY-SSW-JSC016).

✉ Xiao-Xiao Li  
 lixiaoxiao@sinap.ac.cn

Xiang-Zhou Cai  
 caixz@sinap.ac.cn

Jin-Gen Chen  
 chenjg@sinap.ac.cn

<sup>1</sup> Shanghai Institute of Applied Physics, Chinese Academy of Sciences, Shanghai 201800, China

<sup>2</sup> CAS Innovative Academies in TMSR Energy System, Chinese Academy of Sciences, Shanghai 201800, China

<sup>3</sup> University of Chinese Academy of Sciences, Beijing 100049, China

|                                   |  |
|-----------------------------------|--|
| Abs                               | Thermal absorption: neutron loss by thermal absorption           |
| $\Sigma_f$                        | Macroscopic fission cross section of fuel material               |
| $\Sigma_\gamma$                   | Macroscopic capture cross section of fuel material               |
| $\nu$                             | Average number of neutrons produced per fission of fuel material |
| $\text{Fiss}_{235\text{U}}$       | Thermal production of $^{235}\text{U}$                           |
| $\text{Abs}_{235\text{U}}$        | Thermal absorption of $^{235}\text{U}$                           |
| $\Delta\text{Abs}_{235\text{U}}$  | Variation in $\text{Abs}_{235\text{U}}$                          |
| $\Delta\text{Fiss}_{235\text{U}}$ | Variation in $\text{Fiss}_{235\text{U}}$                         |
| $\sigma_{f,235\text{U}}$          | Microscopic fission cross section of $^{235}\text{U}$            |
| $\text{Abs}_{238\text{U}}$        | Thermal absorption of $^{238}\text{U}$                           |
| $\text{Abs}_{\text{HM}}$          | Thermal absorption of heavy metal                                |
| $\text{Abs}_{\text{FLiBe}}$       | Thermal absorption of light elements in fuel salt                |
| $\text{Abs}_{\text{Grap}}$        | Thermal absorption of graphite                                   |
| $\text{Abs}_{\text{Mod}}$         | Thermal absorption of graphite moderator                         |
| $\text{Abs}_{\text{Refl}}$        | Thermal absorption of graphite reflector                         |
| $\sigma_{a,235\text{U}}$          | Microscopic absorption cross section of $^{235}\text{U}$         |
| $\alpha_{\text{TF}}$              | Symbol for FSTC  |

## 1 Introduction

A liquid-fueled molten salt reactor (MSR) [1] with a thermal neutron spectrum usually takes nuclear graphite as a moderator. This has been implemented in the designs of some pioneering MSRs, such as the molten salt reactor experiment (MSRE) [2] and the molten salt breeder reactor (MSBR) [3]. The thermal expansion of graphite is a complex phenomenon, and the expansion coefficient depends strongly on its temperature, form, and direction [4]. As the graphite-moderator temperature increases, the thermal neutron scattering results in a shift of the Maxwellian component to a higher energy region and, therefore, the neutron spectrum becomes harder [5, 6]. A reactivity change in the core is then introduced. Through reassessments of the MSBR [7], the negative total temperature coefficient of reactivity (TCR) is very weak ( $-2.0$  pcm/K) owing to its slightly positive moderator temperature coefficient of reactivity (MTC).

Most previous studies have concentrated on geometry variations to improve the TCR, including the fuel salt temperature coefficient of reactivity (FSTC) and the MTC, especially the latter one. Mathieu et al. [8, 9] investigated the effects of geometry variations on the TCR, including the fuel channel radius, the graphite hexagon size, and the fuel salt volume. Nagy [10, 11] then took into account

several variations, including the fuel channel diameter, the graphite-moderator volume, the thorium concentration, and the power density and provided a core design consideration to achieve a sufficiently negative TCR and better breeding performance. Additionally, Křepel et al. carried out detailed research on the effects of salt-to-graphite ratio on the TCR by fixing the fuel salt composition and graphite assembly size [12]. The effects of salt-to-graphite ratio under different graphite assembly sizes were investigated by Zou et al. [13]. Based on the above analyses, it can be concluded that more homogenized cores together with smaller fuel channels and/or a larger graphite-moderator volume can obtain a more negative TCR with a sufficiently negative or less positive MTC.

Besides the geometry factor, different fuel salt compositions with different chemical and physical properties, such as density, volume expansion coefficient, thermal conductivity, and thermal capacity [14] have a direct influence on neutronic characteristics, such as breeding capability, neutron moderation, fissile inventory as well as the TCR. In previous studies, the effects of fuel salt composition were assessed on the bases of thermal-hydraulic and economic analyses [15]. The coolant density coefficient for different carrier salts (chlorides, fluorides, etc.) was compared without physical explanations [16]. The heavy metal (HM) proportion in the salt mixture and the fissile ( $^{235}\text{U}$  for uranium fuel) enrichment were adjusted in the MSRE and displayed different magnitudes of the TCR [17]. The total feedback coefficient at equilibrium for different HM proportions in a  $^{233}\text{U}$ -started thorium molten salt reactor (TMSR) configuration was then evaluated [18]. Moreover, the integral molten salt reactor (IMSR) proposed by a company called terrestrial energy has evaluated the TCR for all combinations of core sizes and fuel salt compositions. However, few studies to provide a detailed mechanism of the impact of fuel salt composition on the TCR have been attempted. It is, therefore, necessary to give a more detailed assessment of the contribution of fuel salt composition to the TCR.

The value of the TCR is the sum of the contribution of the fuel salt (i.e., the FSTC) and the graphite moderator (i.e., the MTC). While the FSTC is strongly negative and immediate, the slow MTC has a smaller negative value and may even be positive, which can affect the stability of core operation over long time scales. A related study concentrating on the FSTC was performed in our previous work [19]. It was shown that the FSTC is mainly caused by the variable neutron spectrum owing to the variations in temperature and density of the fuel salt in the core. To obtain a more comprehensive analysis of the TCR in terms of  $^{235}\text{U}$  enrichment and HM proportion, this work emphasizes the MTC, which is primarily induced through the neutron

energy shift from the temperature change in the graphite moderator. The essential six-factor formula on a core level is still introduced to describe the effects of MTC quantitatively in this work.

In this study, the contributions of  $^{235}\text{U}$  enrichment and HM proportion to the MTC are investigated. The descriptions of the reactor core, the fuel salt composition, the calculation of the MTC, and the calculation tool are provided in Sect. 2. The contributions of  $^{235}\text{U}$  enrichment for different HM proportions to the MTC from the perspective of the six-factor formula are discussed in Sect. 3. Finally, the conclusions are drawn in Sect. 4.

## 2 Analysis methodology

### 2.1 Simulation model specifications

The reactor core of the graphite-moderated MSR used in this study (see Fig. 1) was cylindrical with a diameter of 300 cm and a height of 300 cm. The core assembly was 260 cm in height and 200 cm in diameter. The axial and radial thicknesses of the graphite reflector were 50 cm and 20 cm, respectively. The core size of 3.0 m resulted in the least neutron leakage and was considered as the limit for road transportation. The reflector thickness was chosen to ensure optimal neutron economy. The core assembly was formed by 1129 graphite fuel elements, each  $5.1 \times 5.1$  cm in cross section and 260-cm long. The graphite fuel elements contained cylindrical fuel cells in the center surrounded by graphite moderators. Fuel salt flowed through the fuel cells with a radius of 1.0 cm. This provided volume fractions of 0.88 for the graphite moderator and 0.12 for the fuel salt in the core assembly region. The graphite fuel cell width of 5.1 cm and the fuel salt fraction of 0.12 were based mainly on the consideration of obtaining a more negative MTC. Control rods are mainly used to cause minor changes in reactivity, such as those required to regulate the

temperature during operation and those for keeping the reactor at a subcritical level. The design requirements for the control rods have not been investigated in detail because the desired requirements are achievable with up to three control rods in the center of the core. The effect of the control rods on the temperature coefficient of reactivity was out of the scope of this study and was not considered.

The fuel salt was comprised of  $\text{LiF}\text{--}\text{BeF}_2\text{--}\text{UF}_4$  owing to its chemical, physical, and favorable neutron absorption properties [20]. Beryllium fluoride was selected to obtain a low melting point. Lithium fluoride (99.95%  $^7\text{Li}$  in  $\text{LiF}$ ) imparted good fluid flow properties to the salt mixture. The uranium fluoride was composed of low enriched uranium and its molar proportion was the HM proportion mentioned previously. The molar ratio of  $\text{LiF}$  was 68 mol% while the remaining 32 mol% included  $\text{UF}_4$  (i.e., the HM proportion listed in Table 1) and  $\text{BeF}_2$ . A reduction in the HM proportion entails an increase in the melting point of the fuel salt. For instance, the melting point increases from 440 to 480 °C when the HM proportion decreases from 12 to 2 mol%. This means that a higher operation temperature is required, which then effects a greater challenge regarding the heat and irradiation resistance of structural materials. Additionally, a higher proportion of carrier salt corresponds to a lower HM proportion, which causes more parasitic neutron captures. In this work, the minimum HM proportion was set to 2 mol%. Moreover, considering the solubility of heavy metals in fluoride salt as well as the oxygen control, the upper limit of the HM proportion was set to 12 mol%. The density and the coefficient of expansion for the fuel salt are also listed in Table 1. It is important to note that the results for  $\text{HM} = 10$  mol%, including the density and expansion coefficient of the fuel salt and the trend of the MTC, are intermediate between  $\text{HM} = 8$  and  $\text{HM} = 12$  mol%. At a fixed  $^{235}\text{U}$  enrichment, the distinction of the MTC between two adjacent HM proportions becomes increasingly smaller as the HM proportion increases. Thus, the data for  $\text{HM} = 10$  mol% are not shown in this article, but this does not affect the major results.

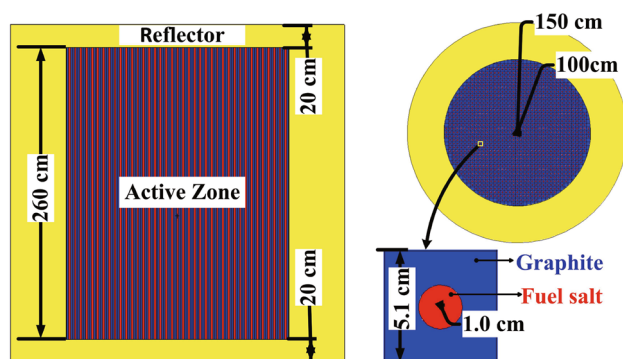


**Fig. 1** A schematic diagram of the reactor core of the MSR used in this study

**Table 1** Density and expansion coefficient of the fuel salt for different HM proportions at 880 K

| HM (mol%) | Density ( $\text{g}/\text{cm}^3$ ) | Expansion coefficient ( $\text{K}^{-1}$ ) |
|-----------|------------------------------------|---|
| 2         | 2.51                               | 2.2736E-04                                |
| 4         | 2.75                               | 2.2364E-04                                |
| 6         | 2.99                               | 2.2016E-04                                |
| 8         | 3.20                               | 2.1690E-04                                |
| 12        | 3.59                               | 2.1095E-04                                |

The mean operating temperature in the core was 880 K. Taking into account nonproliferation, the  $^{235}\text{U}$  enrichment was kept under 20%. Taking the neutron economy into consideration, the  $^7\text{Li}$  enrichment in LiF was set to 99.95%. The graphite density for both the moderator and the reflector was  $1.86\text{ g/cm}^3$ . The  $^{235}\text{U}$  enrichment and HM proportion have direct and significant influences on the neutron spectrum, and thus, on the MTC. More detailed discussions can be found in Sect. 3.

## 2.2 Calculation of the MTC

The MTC (denoted by  $\alpha_{\text{TM}}$ ) is defined as the change in the reactivity ( $\rho$ ) per degree change in the graphite-moderator temperature (labeled as “TM”). That is, the MTC is the derivative of  $k$  with respect to TM and calculated using the following equation:

$$\alpha_{\text{TM}} = \frac{d\rho}{d\text{TM}} = \frac{1}{k} \frac{dk}{d\text{TM}}, \quad (1)$$

where  $k$  is the effective multiplication factor. To ensure calculation accuracy, five temperature points (680, 780, 880, 980, and 1080 K) are used in the calculation of the MTC. In order to obtain a quantified MTC, the classical six-factor formula [21, 22] is introduced to describe  $k$ , which is calculated by

$$k_{\text{eff}} = \varepsilon p \eta f P_{\text{FNL}} P_{\text{TNL}} = \varepsilon p \eta f A, \quad (2)$$

where  $\varepsilon$  denotes the fast fission factor,  $p$  denotes the resonance escape probability,  $\eta$  denotes the thermal reproduction factor,  $f$  denotes the thermal utilization factor, and  $P_{\text{FNL}}(P_{\text{TNL}})$  denotes the fast (thermal) non-leakage probability. To reduce unnecessary complexity, the total non-leakage probability ( $A$ ) is defined as the multiplication of  $P_{\text{FNL}}$  and  $P_{\text{TNL}}$ . Therefore, five factors (including  $\varepsilon$ ,  $p$ ,  $\eta$ ,  $f$ , and  $A$ ) are adopted to describe the variations in the MTC in the following sections.

From the perspective of the six-factor formula, the MTC is divided into five components, including  $\alpha_{\text{TM}}(\varepsilon)$ ,  $\alpha_{\text{TM}}(p)$ ,  $\alpha_{\text{TM}}(\eta)$ ,  $\alpha_{\text{TM}}(f)$ , and  $\alpha_{\text{TM}}(A)$ , and is calculated by

$$\begin{aligned} \alpha_{\text{TM}} &= \alpha_{\text{TM}}(\varepsilon) + \alpha_{\text{TM}}(p) + \alpha_{\text{TM}}(\eta) + \alpha_{\text{TM}}(f) + \alpha_{\text{TM}}(A) \\ &= \frac{1}{\varepsilon} \frac{d\varepsilon}{d\text{TM}} + \frac{1}{p} \frac{dp}{d\text{TM}} + \frac{1}{\eta} \frac{d\eta}{d\text{TM}} + \frac{1}{f} \frac{df}{d\text{TM}} + \frac{1}{A} \frac{dA}{d\text{TM}}, \end{aligned} \quad (3)$$

where TM changes from 680 to 1080 K in steps of 100 K. For simplicity, an isothermal temperature is used in the calculation of the MTC.

The MCNP5 code cannot directly give the cross section used in the calculation for each factor in the six-factor formula. Hence, the F4 card and the FM card were implemented in the input file. The F4 card is used to

calculate the flux averaged over a cell. The FM card is a tally multiplier card and is used to calculate the average nuclear reaction rate. The MCNP cross section library reaction numbers used in the FM card were  $-2$  for an absorption reaction,  $-6$  for a total fission reaction, and  $-7$  for fission  $\nu$ . An E4 card was added to create energy bins for the thermal neutron region ( $< 0.625\text{ eV}$ ) and the fast neutron region ( $0.625\text{ eV}$ – $20\text{ MeV}$ ).

## 2.3 Computational tool

The calculations presented in this article were performed with the MCNP5 code on the core level. In order to perform accurate calculations with the uranium-based fuel, a compact ENDF (ACE) format cross section library with continuous energy was selected from the ENDF/B-VII library. To improve the accuracy of the results, each criticality calculation was scheduled to skip 50 cycles and run a total of 200 cycles with nominally one million neutrons per cycle. The typical computing time for one criticality calculation was about 7 h with 16-point parallel computing.

## 3 Results and discussion

Theoretically, similar to the FSTC, the MTC can also be separated into the reactivity effects of temperature and expansion (i.e., density). Nevertheless, the expansion of solid graphite is a complex phenomenon, and the graphite expansion coefficient may strongly depend on its temperature and irradiated fluence [12], where the latter effect is only considered for neutron irradiation over a long period. More importantly, the density change in graphite within a short operational time span owing to expansion is negligible compared to that for liquid fuel salt. Therefore, the MTC investigated in this work is limited to the reactivity effect of pure temperature. In the calculations, the MTC was simulated by a 100 K increment of the graphite-moderator temperature, while the density and temperature of the fuel salt were kept at nominal levels with a mean temperature of 880 K. Meanwhile, the core geometry and the graphite-moderator density were kept constant.

### 3.1 Effects of $^{235}\text{U}$ enrichment and HM proportion on the MTC

#### 3.1.1 Neutron spectrum

For neutrons with energies of the order of eV or lower, the target nucleus cannot be considered stationary because the neutron energy is comparable to the kinetic energy of

the thermal motion of the scattering target nucleus. When an elastic collision occurs between the neutron and the scattering target nucleus, the neutron may obtain energy from the vibration of the scattering nucleus. Hence, the energy of the outgoing neutron may be larger than that of the incident neutron, which is the phenomenon of neutron upward scattering in the thermal energy region [23]. With an increase in the graphite-moderator temperature, the vibration of the graphite nucleus becomes violent, the neutron obtains energy from the graphite nucleus more easily, and the upward scattering effect becomes more obvious. The Maxwellian component then shifts to a higher energy region, the neutron spectrum becomes harder, and the graphite moderator's ability to slow the neutrons down weakens.

Figure 2 gives the neutron spectra for two different graphite-moderator temperatures (880 K and 980 K). The spectra are normalized to their respective total number of counts in the energy range from  $1\text{E}-09$  to  $20\text{ MeV}$ . It can be seen that the neutron energy shifts with a slight increase in the normalized flux values. More importantly, the neutron spectrum hardening mostly occurs below  $1\text{ eV}$ , and there is an intersection point of the neutron spectrum curves for different temperatures around  $0.16\text{ eV}$ . The stronger the slowing ability of the graphite, the more obvious the Maxwellian component, the more apparent the hardening of the neutron spectrum, and the greater the magnitude of the MTC. The sign (“+” or “−”) of the MTC is primarily dependent on the distance between two adjacent fuel cells. Through research, this distance should be less than about  $15\text{ cm}$  to obtain a negative MTC. Such an investigation involves the influence of the geometry of the graphite fuel cell on the MTC, which is out of the scope of this article and not discussed here. Hence, for the graphite fuel cell used in this work, the distance was  $3.1\text{ cm}$  corresponding to a negative MTC.

To describe the neutron spectrum quantitatively, a spectrum factor defined as the energy of average lethargy

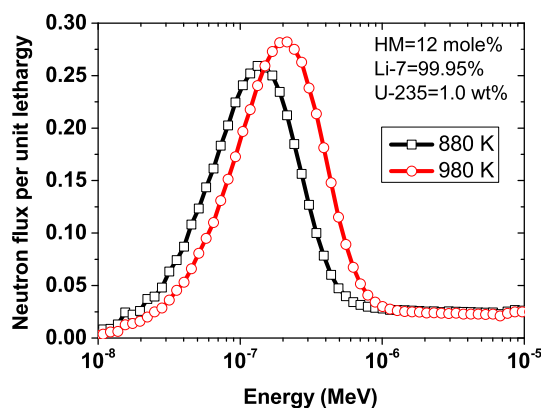


Fig. 2 Neutron energy shift with changing moderator temperature

of fission (EALF) is introduced. A larger EALF represents a harder neutron spectrum. EALF is defined using the following equations [24] and calculated by MCNP5:

$$\text{EALF} = \frac{E_0}{e^{\bar{u}}}, \quad (4)$$

$$\bar{u} = \frac{\sum_m \sum_g \bar{u}_g \Phi_{g,m} \Sigma_{f,g,m}}{\sum_m \sum_g \Phi_{g,m} \Sigma_{f,g,m}}, \quad (5)$$

where  $E_0$  is the maximum energy considered ( $10\text{ MeV}$ ),  $m$  is the index for material regions,  $g$  is the index for energy groups,  $\bar{u}_g$  is the average lethargy for energy group  $g$ ,  $\Phi_{g,m}$  is the neutron flux in the material region  $m$  and the energy group  $g$ , and  $\Sigma_{f,g,m}$  is the macroscopic fission cross section in the region  $m$  and the energy group  $g$ .

Figure 3 shows the EALF as a function of  $^{235}\text{U}$  enrichment and HM proportion. It can be seen that a higher  $^{235}\text{U}$  enrichment and/or a higher HM proportion has a larger EALF corresponding to a harder neutron spectrum. Furthermore, the EALF is more sensitive to the change in the  $^{235}\text{U}$  enrichment for a higher HM proportion. The lower the HM proportion, the smaller the increment of the EALF owing to the increasing  $^{235}\text{U}$  enrichment. For instance, as the  $^{235}\text{U}$  enrichment increases from  $1$  to  $20\text{ wt\%}$ , the EALF increases by  $7.9$  times and  $1.6$  times for  $\text{HM} = 12\text{ mol\%}$  and  $\text{HM} = 2\text{ mol\%}$ , respectively. Similarly, the lower  $^{235}\text{U}$  enrichment presents a smaller increment in the EALF on account of the increasing HM proportion. For example, when the HM proportion increases from  $2$  to  $12\text{ mol\%}$ , the EALF increases by  $1.4$  times and  $6.8$  times for a  $^{235}\text{U}$  enrichment equal to  $1\text{ wt\%}$  and  $20\text{ wt\%}$ , respectively. In other words, it is conducive to alter the neutron spectrum by adjusting the  $^{235}\text{U}$  enrichment for a higher HM proportion or changing the HM proportion for a higher  $^{235}\text{U}$  enrichment.

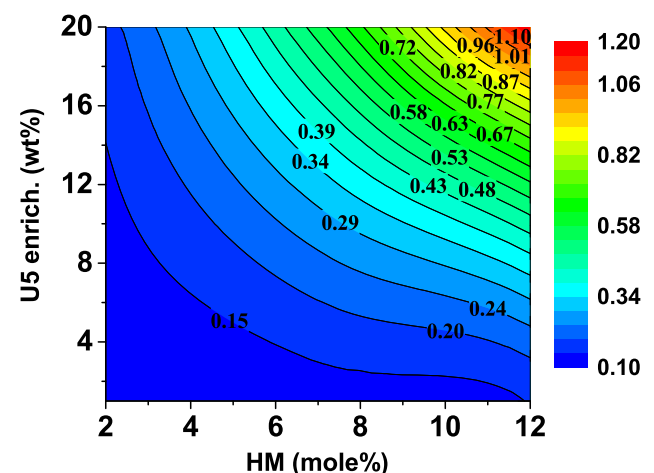


Fig. 3 EALF as a function of  $^{235}\text{U}$  enrichment and HM proportion



There are two highlights. First, for a fixed graphite fuel element, the sign of the MTC is related to the type of nuclear fuel. As the graphite-moderator temperature increases, the Maxwellian component shifts to higher energies, the neutron spectrum becomes harder, and the average thermal absorption (capture and fission) cross section of nuclides, such as  $^{235}\text{U}$ ,  $^{238}\text{U}$ , graphite, and FLiBe, decreases and makes a positive contribution to the MTC. The term “FLiBe” is used here to include  $^{19}\text{F}$ ,  $^6\text{Li}$ ,  $^7\text{Li}$ , and  $^9\text{Be}$ . Different nuclides have different decrements in their respective thermal absorption cross section, which are mainly related to the distance between two adjacent fuel cells. A negative or a positive MTC is then presented. Second, the magnitude of the MTC is mainly dependent on the neutron spectrum shape, such as the degree of thermalization or hardness. As the neutron spectrum hardens owing to the increasing  $^{235}\text{U}$  enrichment and/or HM proportion, the percentage of thermal neutrons decreases, compounded by the fact that the increasing graphite-moderator temperature mainly affects the thermal region, the contributions of thermal absorption, and total absorption of the nuclides to the MTC weaken. The following discussions are based on the above two points. It should also be noted that the neutron energy in the thermal region is less than 0.625 eV.

### 3.1.2 Contributions of $\alpha_{\text{TM}}(\varepsilon)$ and $\alpha_{\text{TM}}(p)$ to the MTC

The temperature coefficient for  $\varepsilon$  ( $\alpha_{\text{TM}}(\varepsilon)$ ) and that for the resonance escape probability ( $\alpha_{\text{TM}}(p)$ ) are strongly affected by the neutron spectrum. As the graphite-moderator temperature increases, the Maxwellian component shifts to higher energies and the neutron spectrum becomes harder, corresponding to a larger EALF (Fig. 2), which then enhances the probability of fast fissions. Thus, a positive  $\alpha_{\text{TM}}(\varepsilon)$  is presented. As mentioned above, the ratio of the moderating atoms (molecules of graphite) owing to the increasing graphite-moderator temperature is neglected. However, an increased graphite-moderator temperature leads to a harder neutron spectrum and results in a decreasing macroscopic scattering cross section for the moderator. The macroscopic slowing-down power of the graphite moderator then weakens, the transport mean free path becomes larger, and more neutrons are absorbed by the nuclear fuel or the moderator in the resonance region. As such, the probability of absorption by the nuclear fuel or the moderator in the thermal region decreases, and a reduction in the resonance escape probability is introduced. Therefore, a negative  $\alpha_{\text{TM}}(p)$  is revealed.

To evaluate the actual contributions of  $\alpha_{\text{TM}}(\varepsilon)$  and  $\alpha_{\text{TM}}(p)$  to the MTC, Fig. 4 presents the variations in  $\alpha_{\text{TM}}(\varepsilon)$  (top) and  $\alpha_{\text{TM}}(p)$  (bottom) with  $^{235}\text{U}$  enrichment for

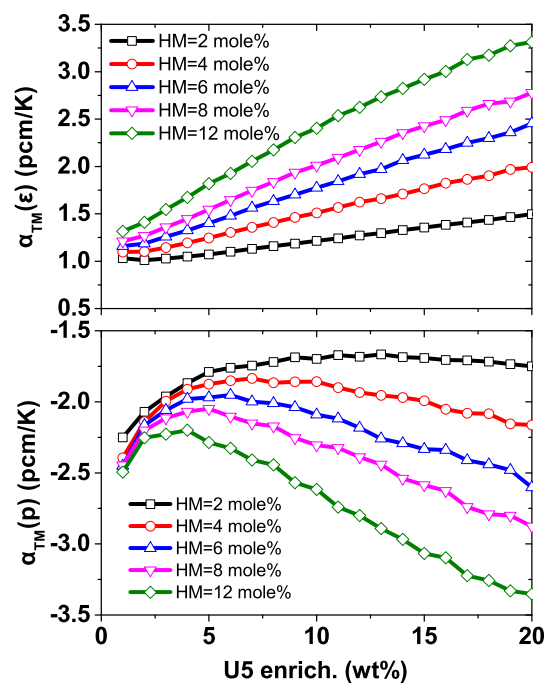


**Fig. 4** Variations in  $\alpha_{\text{TM}}(\varepsilon)$  (top) and  $\alpha_{\text{TM}}(p)$  (bottom) with  $^{235}\text{U}$  enrichment for different HM proportions

different HM proportions. We will discuss each of them in turn.

First, the magnitude of  $\alpha_{\text{TM}}(\varepsilon)$  [Fig. 4 (top)] is mainly dependent on the neutron spectrum shape. The main contributions to  $\alpha_{\text{TM}}(\varepsilon)$  are the thermal fission (neutron energy  $E < 0.625$  eV) and the total fission ( $1 \times 10^{-9}$  eV  $< E < 20$  MeV) of heavy metal (mainly  $^{235}\text{U}$ ). As discussed before, the increasing graphite-moderator temperature leads to a reduction in both thermal fission and total fission. This means that both thermal fission and total fission have positive effects on  $\alpha_{\text{TM}}(\varepsilon)$ . As the  $^{235}\text{U}$  enrichment or the HM proportion increases, the neutron spectrum becomes harder, and the contribution of thermal fission and total fission decrease gradually. The decrement of the contribution of total fission is slower than that of thermal fission owing to the decreasing percentage of thermal fission of  $^{235}\text{U}$ . An increasing  $\alpha_{\text{TM}}(\varepsilon)$  is then revealed. That is, the magnitude of the positive  $\alpha_{\text{TM}}(\varepsilon)$  increases gradually with the increasing  $^{235}\text{U}$  enrichment and/or HM proportion.

Second, differences in the magnitude of  $\alpha_{\text{TM}}(p)$  [Fig. 4 (bottom)] are owing to accumulation effects of neutron spectrum shape as well as the  $^{235}\text{U}$  enrichment and HM proportion. As the Maxwellian component shifts to higher energies and the neutron spectrum becomes harder owing to the increasing graphite-moderator temperature, the thermal absorption for all materials in the core, including the heavy metal (i.e.,  $^{235}\text{U}$  and  $^{238}\text{U}$ ), graphite, and FLiBe decreases in addition to their respective total absorption.

They all make a positive contribution to  $\alpha_{\text{TM}}(p)$ . As the neutron spectrum hardens owing to the increasing  $^{235}\text{U}$  enrichment and/or the HM proportion, the positive contribution of thermal absorption and total absorption of the nuclides to  $\alpha_{\text{TM}}(p)$  decreases. For  $^{235}\text{U}$  and FLiBe, the contribution to  $\alpha_{\text{TM}}(p)$  decreases more slowly in thermal absorption than in total absorption. This is mainly owing to the decrease in the thermal region ( $^{235}\text{U}$  and FLiBe) or the enhancement of the resonance absorption effect (especially  $^{235}\text{U}$ ). Thus, the contribution of  $^{235}\text{U}$  and FLiBe to  $\alpha_{\text{TM}}(p)$  increases with the hardening neutron spectrum. However, for  $^{238}\text{U}$ , the increasing fast fission effect makes up for the decrease in the contribution of the total absorption. This results in a faster decrease in the contribution of thermal absorption than that of the total absorption. A gradually weakening contribution of  $^{238}\text{U}$  to  $\alpha_{\text{TM}}(p)$  is then introduced. In this way, the heavy metal, including  $^{235}\text{U}$  and  $^{238}\text{U}$ , has a positive contribution to  $\alpha_{\text{TM}}(p)$ , and its contribution initially decreases mainly owing to the weakening contribution of  $^{238}\text{U}$  and then increases mainly owing to the increasing contribution of  $^{235}\text{U}$  as the neutron spectrum hardens. Taken together, the variation in the magnitude of  $\alpha_{\text{TM}}(p)$  with  $^{235}\text{U}$  enrichment is primarily dependent on the contribution of heavy metal. That is, at a fixed HM proportion, the magnitude of  $\alpha_{\text{TM}}(p)$  decreases initially and then increases with the increase in the  $^{235}\text{U}$  enrichment. Meanwhile, the difference in the magnitude of  $\alpha_{\text{TM}}(p)$  between different HM proportions mainly depends on the contribution of FLiBe. With the increase in the HM proportion, the magnitude of  $\alpha_{\text{TM}}(p)$  monotonically increases.

Moreover, it is worth mentioning that  $\alpha_{\text{TM}}(\varepsilon)$  and  $\alpha_{\text{TM}}(p)$  show an almost similar magnitude but with opposite signs. This also means that the contributions of  $\varepsilon$  and  $p$  to the MTC compensate for each other.

### 3.1.3 Contribution of $\alpha_{\text{TM}}(\eta)$ to the MTC

The temperature coefficient for  $\eta$  ( $\alpha_{\text{TM}}(\eta)$ ) is closely related to the ratio of the thermal production ( $\text{Fiss} = \sum_f \cdot \nu$ ) to the thermal absorption ( $\text{Abs} = \sum_f + \sum_\gamma$ ) of the fuel material. Here,  $\sum_f$  and  $\sum_\gamma$  are the macroscopic fission and absorption cross sections of fuel material, while  $\nu$  is the average number of neutrons produced per fission. As the graphite-moderator temperature increases, the variation in  $\eta$  is mainly owing to the following two aspects. First, because the changes in the thermal production/absorption of  $^{238}\text{U}$  are much less than in those of  $^{235}\text{U}$ , the variation in  $\eta$  mainly stems from  $^{235}\text{U}$ . In addition,  $\sum_f$  is much larger than  $\sum_\gamma$  for  $^{235}\text{U}$ , and the value of  $\nu$  is usually higher than 2. Hence, the change in  $\text{Fiss}_{235\text{U}}$  (the thermal production of  $^{235}\text{U}$ ) is much larger than that of  $\text{Abs}_{235\text{U}}$  (thermal

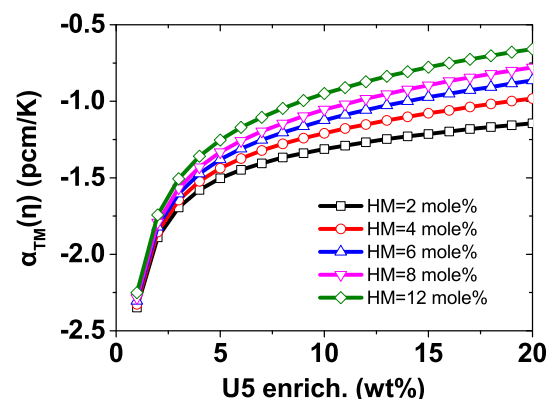
absorption of  $^{235}\text{U}$ ). The hardening neutron spectrum weakens  $\text{Fiss}_{235\text{U}}$  and  $\text{Abs}_{235\text{U}}$ , and thus, a reduction in  $\eta$  is introduced. Second, the Maxwellian component shifts to higher energies, the neutron spectrum becomes harder, and then the average thermal neutron energy increases. Since the fissile material is all  $^{235}\text{U}$  in this work,  $\eta$  will decrease as the neutron energy increases, especially in the thermal neutron ranges ( $< 1 \text{ eV}$ ) [25]. Both of the above two aspects lead to a negative  $\alpha_{\text{TM}}(\eta)$ .

Figure 5 presents the variation in  $\alpha_{\text{TM}}(\eta)$  with  $^{235}\text{U}$  enrichment for different HM proportions. The magnitude of  $\alpha_{\text{TM}}(\eta)$  is mainly related to the neutron spectrum shape and its main contributions, including its thermal production and thermal absorption, are from  $^{235}\text{U}$ . As mentioned previously, both the thermal production and thermal absorption have positive contributions to  $\alpha_{\text{TM}}(\eta)$ , and their contributions decrease as the neutron spectrum hardens. However, because the thermal fission cross section is nearly an order of magnitude lower than the thermal capture cross section, while the average fission neutron number ( $\nu$ ) is larger than 2, the contribution of thermal production decreases faster than that of thermal absorption as the neutron spectrum hardens. A decrease in the magnitude of  $\alpha_{\text{TM}}(\eta)$  is then presented. That is, a lower  $^{235}\text{U}$  enrichment and/or a lower HM proportion results in a stronger  $\alpha_{\text{TM}}(\eta)$ .

### 3.1.4 Contribution of $\alpha_{\text{TM}}(f)$ to the MTC

For a graphite-moderated MSR, the thermal utilization factor ( $f$ ) is calculated by

$$f = \frac{\text{Abs}_{\text{HM}}}{\text{Abs}_{\text{HM}} + \text{Abs}_{\text{FLiBe}} + \text{Abs}_{\text{Grap}}} = \frac{1}{1 + \frac{\text{Abs}_{\text{FLiBe}}}{\text{Abs}_{\text{HM}}} + \frac{\text{Abs}_{\text{Grap}}}{\text{Abs}_{\text{HM}}}}, \quad (6)$$



**Fig. 5** Variation in  $\alpha_{\text{TM}}(\eta)$  with  $^{235}\text{U}$  enrichment for different HM proportions

where “Abs” represents the thermal absorption, while the subscripts HM, FLiBe, and Grap correspond to heavy metal, light elements in fuel salt (including fluorine, lithium, and beryllium), and graphite, respectively. The graphite here includes the moderator and reflector. As the graphite-moderator temperature increases, the hardening neutron spectrum weakens the thermal absorption of the fuel salt and the graphite moderator. That is,  $Abs_{HM}$ ,  $Abs_{FLiBe}$ , and  $Abs_{Mod}$  (the thermal absorption of the graphite moderator) show decreasing trends. The evaluated nuclear data file on the website (<https://www-nds.iaea.org/exfor/endl.htm>) shows that the microscopic absorption cross section of  $^{235}\text{U}$  decreases faster with increasing neutron energy than the other elements, including  $^{238}\text{U}$ , graphite (i.e.,  $^{12}\text{C}$ ), fluorine, lithium, and beryllium, especially in the thermal regions ( $< 1\text{ eV}$ ). The cross section of several important nuclides is presented in Fig. 6. Thus, the decrement of  $Abs_{HM}$  is larger than that of  $Abs_{FLiBe}$ . The ratio of  $Abs_{FLiBe}$  to  $Abs_{HM}$  will increase. Moreover, because the thermal absorption of the graphite reflector ( $Abs_{Ref}$ ) strengthens owing to more fast neutrons leaking from the active core and the calculations indicate that the increment of  $Abs_{Ref}$  is faster than the decrement of  $Abs_{Mod}$ ,  $Abs_{Grap}$  will increase. Combining the decreased  $Abs_{HM}$ , the ratio of  $Abs_{Grap}$  to  $Abs_{HM}$  increases. Above all, a reduction in  $f$  is introduced, and a negative  $\alpha_{TM}(f)$  is shown. It should be especially explained that the possibility of the sign of  $\alpha_{TM}(f)$  being positive is significant for a large graphite assembly size, which results in a positive  $\alpha_{TM}(f)$ . The effects of geometric factors, such as fuel salt fraction and graphite assembly cell size on the temperature coefficient are outside the scope of this article and are not discussed here.

Figure 7 presents the variation in  $\alpha_{TM}(f)$  with  $^{235}\text{U}$  enrichment for different HM proportions. The magnitude of  $\alpha_{TM}(f)$  is mainly related to the neutron spectrum shape.

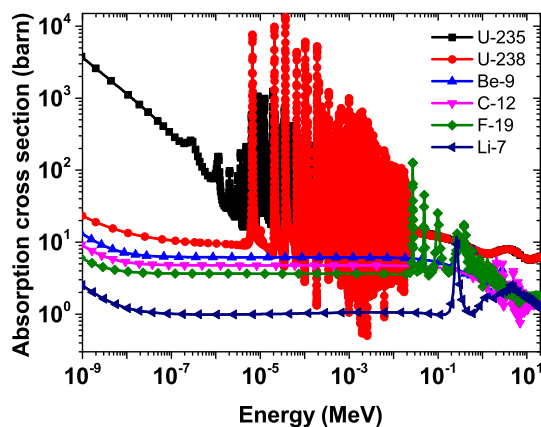


Fig. 6 Absorption cross section for several important nuclides

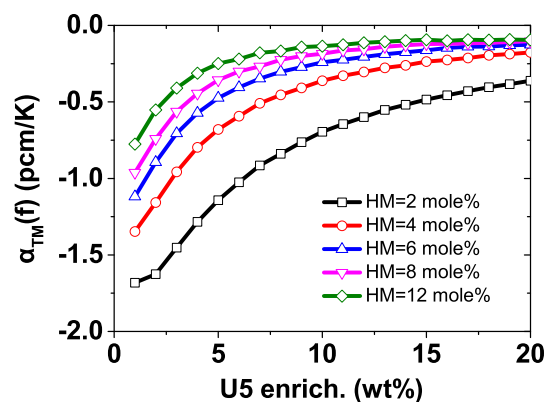


Fig. 7 Variation in  $\alpha_{TM}(f)$  with  $^{235}\text{U}$  enrichment for different HM proportions

When the graphite-moderator temperature increases, the neutron spectrum hardening occurs mainly in the region where the neutron energy is less than 1 eV. In this region, the fastest decrease in the absorption cross section of the nuclides is  $^{235}\text{U}$ , followed by  $^7\text{Li}$ , and then  $^9\text{Be}$ ,  $^{238}\text{U}$ ,  $^{12}\text{C}$ , and  $^{19}\text{F}$  (Fig. 6). In the reactor core, the thermal absorption change in heavy metals mainly comes from  $^{235}\text{U}$ , while that of non-heavy metals (including FLiBe, the moderator, and the reflector) mainly comes from FLiBe (but especially  $^7\text{Li}$ ). As mentioned in Sect. 3.1.2, with the increase in  $^{235}\text{U}$  enrichment and HM proportion, the neutron spectrum hardens and the contribution of  $^{235}\text{U}$  and FLiBe to  $\alpha_{TM}(f)$  decreases. It can be seen from the cross section (Fig. 6) that when the neutron energy is between  $1\text{E}-8$  and  $1\text{E}-6\text{ MeV}$ , the decrease in the rate of absorption cross section of  $^{235}\text{U}$  with neutron energy is obviously faster than that of any nuclide in FLiBe. The positive contribution of  $^{235}\text{U}$  to  $\alpha_{TM}(f)$ , therefore, decreases faster with the hardening neutron spectrum than FLiBe. In short, the harder the neutron spectrum, the smaller the magnitude of  $\alpha_{TM}(f)$ . That is, a lower HM proportion and/or a lower  $^{235}\text{U}$  enrichment results in a higher magnitude of the negative  $\alpha_{TM}(f)$ .

### 3.1.5 Contribution of $\alpha_{TM}(\lambda)$ to the MTC

The distance traveled by fast neutrons during moderation (the slowing-down length) and the distance traveled by thermal neutrons during diffusion (the neutron diffusion length,  $L$ ) in a reactor are important in reactor design because of their effects on the neutron leakage. The first directly affects the fast non-leakage probability ( $P_{FNL}$ ), while the second directly influences the thermal non-leakage probability ( $P_{TNL}$ ). For the graphite-moderated MSR used in this work, the neutron diffusion length was much larger than the slowing-down length. Therefore, the temperature coefficient for  $\lambda$ , ( $\alpha_{TM}(\lambda)$ ), was linked closely



with the neutron diffusion length rather than the slowing-down length. A larger neutron diffusion length results in a reduction in  $P_{\text{TNL}}$ , and then a decreasing  $\Lambda$  is presented. Because the neutron diffusion length is dependent on the macroscopic cross section for elastic scattering ( $\Sigma_s$ ) and the macroscopic cross section for neutron absorption ( $\Sigma_a$ ), i.e.,  $L^2 \propto \frac{1}{\Sigma_s \Sigma_a}$ , we will study the impact of the change in graphite-moderator temperature on these two processes. As the graphite-moderator temperature increases,  $\Sigma_a$  decreases owing to the hardening neutron spectrum. Meanwhile, because the microscopic scattering cross section is almost independent of neutron energies, especially for low-energy neutrons, and the atomic density of solid graphite is nearly invariable, the value of  $\Sigma_s$  shows little change. That is, the above two processes make  $L^2$  greater. Therefore, as the graphite-moderator temperature increases, the neutron diffusion length increases, and the thermal non-leakage probability then decreases corresponding to a reduction in the total non-leakage probability ( $\Lambda$ ). Thus, a negative  $\alpha_{\text{TM}}(\Lambda)$  is introduced.

Figure 8 presents the variation in  $\alpha_{\text{TM}}(\Lambda)$  with  $^{235}\text{U}$  enrichment for different HM proportions. Other than the neutron spectrum shape, the magnitude of  $\alpha_{\text{TM}}(\Lambda)$  is mainly related to heavy metals, including the HM proportion and  $^{235}\text{U}$  enrichment. At a fixed  $^{235}\text{U}$  enrichment, a decreasing HM proportion leads to a decrease in the neutron absorption of heavy metals. At a fixed HM proportion, because the absorption cross section of  $^{235}\text{U}$  is much higher than that of  $^{238}\text{U}$  (Fig. 6), a decreasing  $^{235}\text{U}$  enrichment also corresponds to a reduction in the neutron absorption of heavy metal. Therefore, as the HM proportion and/or the  $^{235}\text{U}$  enrichment decreases, the neutron leakage increases owing to the reducing neutron absorption of the heavy metal. A large variation in neutron leakage will then be induced, and even the graphite-moderator temperature will change slightly. It, therefore, means that the magnitude of

$\alpha_{\text{TM}}(\Lambda)$  increases as  $^{235}\text{U}$  enrichment and/or HM proportion decrease.

### 3.1.6 The MTC as a function of $^{235}\text{U}$ enrichment for different HM proportions

Based on the above discussions, one knows that the MTC is presented as a combination of the temperature effects of five factors. The sign of  $\alpha_{\text{TM}}(\varepsilon)$  is positive, while the other four are negative. To ensure a negative MTC, one usually suppresses the positive  $\alpha_{\text{TM}}(\varepsilon)$  and the possible positive  $\alpha_{\text{TM}}(f)$  in the design of the MSR core. It is also significant that the sign of the MTC is closely related to the nuclear fuel type, while the magnitude of the MTC is primarily dependent on the neutron spectrum shape.

The variation in the MTC with  $^{235}\text{U}$  enrichment for different HM proportions is shown in Fig. 9. It can be found that the MTC can remain negative for all of the selected  $^{235}\text{U}$  enrichments and HM proportions for the MSR core chosen in this work. As mentioned above, the signs of  $\alpha_{\text{TM}}(\varepsilon)$  and  $\alpha_{\text{TM}}(p)$  are opposite while their magnitudes are very similar, and so, these two temperature coefficients approximately compensate for each other. Thus, the trends of the MTC with  $^{235}\text{U}$  enrichment depend primarily on  $\alpha_{\text{TM}}(\eta)$ ,  $\alpha_{\text{TM}}(\Lambda)$ , and  $\alpha_{\text{TM}}(f)$ . The magnitudes of the MTC for different HM proportions decrease monotonously as the  $^{235}\text{U}$  enrichment increases. Meanwhile, at a fixed  $^{235}\text{U}$  enrichment, a lower HM proportion presents a more negative MTC. That is, a soft neutron spectrum is beneficial to obtain a more negative MTC.

### 3.2 Impacts of $^{235}\text{U}$ enrichment and HM proportion on the TCR

In order to reveal the impact of  $^{235}\text{U}$  enrichment and HM proportion on the TCR fully, their contributions to the

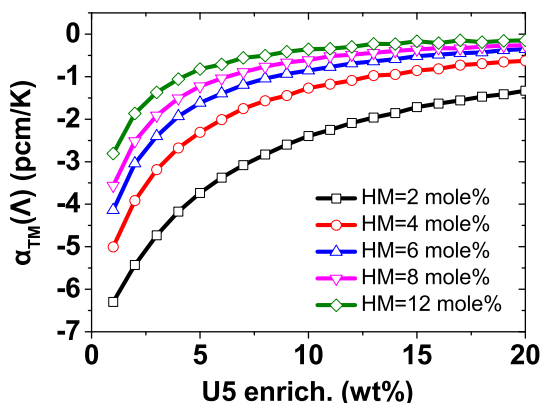


**Fig. 8** Variation in  $\alpha_{\text{TM}}(\Lambda)$  with  $^{235}\text{U}$  enrichment for different HM proportions

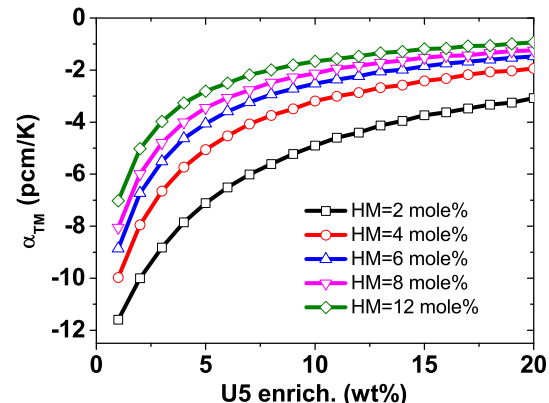


**Fig. 9** Variations in the MTC with  $^{235}\text{U}$  enrichment for different HM proportions

FSTC and the MTC are combined. The FSTC (denoted by  $\alpha_{TF}$ ) is also a combined result of the Doppler coefficient and the density coefficient, which are mainly attributed to  $\alpha_{TF}(\varepsilon)$  and  $\alpha_{TF}(p)$ , respectively, for an under-moderated MSR. As the fuel salt temperature increases, the Doppler broadening leads to a decreasing resonance escape probability corresponding to a negative  $\alpha_{TF}(p)$  and results in an increasing fast fission factor corresponding to a positive  $\alpha_{TF}(\varepsilon)$ . Meanwhile, the reducing fuel salt density results in a softer neutron spectrum and subsequently causes an increasing resonance escape probability and a decreasing fast fission factor, corresponding to a positive  $\alpha_{TF}(p)$  and a negative  $\alpha_{TF}(\varepsilon)$ , respectively. Since the magnitude of  $\alpha_{TF}(p)$  is always higher than that of  $\alpha_{TF}(\varepsilon)$ , the sign of the Doppler coefficient is negative, while that of the density coefficient is positive for an under-moderated core. Nevertheless, for an over-moderated MSR, the magnitude of the negative  $\alpha_{TF}(f)$  of the density coefficient is greater than the other three and leads to a negative density coefficient. Consequently, the sign of the FSTC is always negative because the magnitude of the negative Doppler coefficient is larger than that of the positive density coefficient for an under-moderated MSR. Unlike the always negative FSTC, however, the MTC might be negative (or positive) owing to the negative (or positive)  $\alpha_{TM}(f)$  for small (or large) distances between two adjacent fuel salt cells. For the graphite fuel cell used in this work, the MTC was always negative, which was mainly attributed to the negative  $\alpha_{TM}(\eta)$ ,  $\alpha_{TM}(f)$ , and  $\alpha_{TM}(A)$ , while ( $\alpha_{TM}(\varepsilon)$  and  $\alpha_{TM}(p)$ ) had similar magnitudes but opposite signs.

The impact of  $^{235}\text{U}$  enrichment and HM proportion on the TCR are shown in Fig. 10. It can be seen that a lower  $^{235}\text{U}$  enrichment and/or a lower HM proportion results in a more negative TCR. The main reasons for this are as follows: First, all the temperature coefficients (especially their respective magnitudes), including the TCR and its two separated parts (the FSTC and the MTC), are closely

related to the neutron spectrum shape. Second, as the neutron spectrum hardens owing to the increasing  $^{235}\text{U}$  enrichment and HM proportion, the magnitude of both the FSTC (mainly influenced by the density coefficient rather than the Doppler coefficient) and the MTC decrease. Finally, the TCR, as a result, is a combination of the FSTC and the MTC, and its magnitude decreases as the neutron spectrum hardens. To summarize, both a low  $^{235}\text{U}$  enrichment and/or a low HM proportion is recommended to obtain a more negative TCR. It is worth noting that the specific value of the TCR also needs the transient analysis together with the control worth of the reactivity control system. This will be very valuable research and will be performed in our future work.

## 4 Summary

In addition to the geometric factor, the fuel salt composition also has a direct and significant influence on the neutron spectrum and then on the TCR, which includes the FSTC and the MTC. Our previous work discussed the effects of fuel salt composition on the FSTC in terms of  $^{235}\text{U}$  enrichment and HM proportion. To obtain a full understanding of the TCR, the effects of the MTC, which might be positive and affect the safety of the reactor operation, are investigated. For the MTC in the reactor core chosen in this work, the contribution of  $\alpha_{TM}(\varepsilon)$  is positive while the other four ( $\alpha_{TM}(p)$ ,  $\alpha_{TM}(\eta)$ ,  $\alpha_{TM}(f)$ , and  $\alpha_{TM}(A)$ ) are negative. The results indicate that a low HM proportion and/or a low  $^{235}\text{U}$  enrichment is favorable in obtaining a more negative MTC. In short, a relatively soft neutron spectrum is beneficial to improve the MTC owing to its increasing  $\alpha_{TM}(\eta)$ ,  $\alpha_{TM}(A)$ , and  $\alpha_{TM}(f)$  (but especially the former two).

For a graphite-moderated MSR, different geometry components, such as the fuel salt fraction and graphite assembly size, present different TCR values. More specifically, the fuel salt density coefficient changes from negative to positive with the increasing fuel salt fraction. In addition, as the graphite assembly size increases, the sign of  $\alpha_{TM}(f)$  of the MTC changes from negative to positive. Therefore, further analysis on the effects of the combination of fuel salt composition and geometry components on the FSTC and the MTC should be performed to obtain a more reasonable TCR for different MSR fuel-moderator configurations from the thermal spectrum to the epithermal spectrum. Moreover, the effects of separate nuclides and burnup on the TCR should also be investigated. It is also essential to study the range of magnitudes for the TCR of an MSR core, which will be carried out in future work.

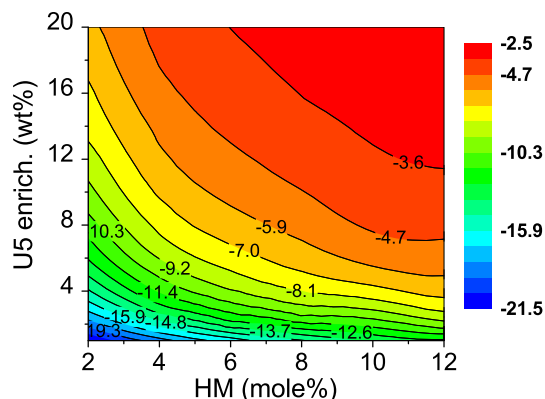


**Fig. 10** The TCR as a function of  $^{235}\text{U}$  enrichment and HM proportion

## References

1. J. Serp, M. Allibert, O. Beneš et al., The molten salt reactor (MSR) in generation IV: overview and perspectives. *Prog. Nucl. Energy* **77**, 308 (2014). <https://doi.org/10.1016/j.pnucene.2014.02.014>
2. R.C. Robertson, *MSRE Design and Operations Report. Part I. Description of Reactor Design* (Oak Ridge National Lab., ORNL-TM-0728, 1965). <https://doi.org/10.2172/4654707>
3. R.C. Robertson, *Conceptual Design Study of a Single-fluid Molten-salt Breeder Reactor* (Oak Ridge National Lab., ORNL-4541, 1971). <https://doi.org/10.2172/4030941>
4. D.K.L. Tsang, B.J. Marsden, S.L. Fok et al., Graphite thermal expansion relationship for different temperature ranges. *Nucl. Technol.* **43**, 2902 (2005). <https://doi.org/10.1016/j.carbon.2005.06.009>
5. J. Žáková, *Analysis of an Advanced Graphite Moderated and Molten Salt Cooled High Temperature Reactor*. Master of Science Thesis (Department of Reactor Physics, Royal Institute of Technology Stockholm, Sweden 2006)
6. D.Y. Cui, S.P. Xia, X.X. Li et al., Transition toward thorium fuel cycle in a molten salt reactor by using plutonium. *Nucl. Sci. Tech.* **28**, 152 (2017). <https://doi.org/10.1007/s41365-017-0303-y>
7. J. Křepel, U. Rohde, U. Grundmann et al., Dynamics of molten salt reactors. *Nucl. Technol.* **164**, 34 (2008). <https://doi.org/10.13182/NT08-A4006>
8. L. Mathieu, D. Heuer, R. Brissota et al., The thorium molten salt reactor: moving on from the MSBR. *Prog. Nucl. Energy* **48**, 664 (2006). <https://doi.org/10.1016/j.pnucene.2006.07.005>
9. L. Mathieu, D. Heuer, E. Merle-Lucotte et al., Possible configurations for the thorium molten salt reactor and advantages of the fast nonmoderated version. *Nucl. Sci. Eng.* **161**, 78 (2009). <https://doi.org/10.13182/NSE07-49>
10. K. Nagy, J.L. Kloosterman, D. Lathouwers et al., New breeding gain definitions and their application to the optimization of a molten salt reactor design. *Ann. Nucl. Energy* **38**, 601 (2011). <https://doi.org/10.1016/j.anucene.2010.09.024>
11. K. Nagy, *Dynamics and Fuel Cycle Analysis of a Moderated Molten Salt Reactor* (Delft University of Technology, Delft, 2012). <https://doi.org/10.4233/uuid:b4d5089d-c2de-446b-94cf-c563dd73e8f1>
12. J. Křepel, B. Hombourger, C. Fiorina et al., Fuel cycle advantages and dynamics features of liquid fueled MSR. *Ann. Nucl. Energy* **64**, 380 (2014). <https://doi.org/10.1016/j.anucene.2013.08.007>
13. C.Y. Zou, X.Z. Cai, D.Z. Jiang et al., Optimization of temperature coefficient and breeding ratio for a graphite-moderated molten salt reactor. *Nucl. Eng. Des.* **281**, 114 (2015). <https://doi.org/10.1016/j.nucengdes.2014.11.022>
14. F. Lantelme, H. Groult, *Molten Salts Chemistry: From Lab to Applications* (Elsevier, Berlin, 2013). <https://doi.org/10.1016/B978-0-12-398538-5.09995-9>
15. D.F. Williams, K.T. Clarno, Evaluation of salt coolants for reactor applications. *Nucl. Technol.* **163**(3), 330 (2008). <https://doi.org/10.13182/NT08-A3992>
16. A. Nuttin, D. Heuer, A. Billebaud et al., Potential of thorium molten salt reactors detailed calculations and concept evolution with a view to large scale energy production. *Prog. Nucl. Energy* **46**, 77 (2005). <https://doi.org/10.1016/j.pnucene.2004.11.001>
17. P.N. Haubenreich, J.R. Engel, B.E. Engel, et al., *MSRE Design and Operations Report. Part III. Nuclear Analysis* (Oak Ridge National Lab., ORNL-TM-0730, 1964). <https://doi.org/10.2172/4114686>
18. E. Merle-Lucotte, D. Heuer, M. Allibert, et al., Optimized transition from the reactors of second and third generations to the thorium molten salt reactor, in *ICAPP 2007: International Congress on Advances in Nuclear Power Plants, May 2007, Nice, France* (American Nuclear Society, in2p3-00135149, 7186, 2007)
19. X.X. Li, Y.W. Ma, C.G. Yu et al., Effects of fuel salt composition on fuel salt temperature coefficient (FSTC) for an under-moderated molten salt reactor (MSR). *Nucl. Sci. Tech.* **29**, 110 (2018). <https://doi.org/10.1007/s41365-018-0458-1>
20. J.R. Keiser, J.H. DeVan, D.L. Manning, *The Corrosion Resistance of Type 316 Stainless Steel to  $\text{Li}_2\text{BeF}_4$*  (Oak Ridge National Lab., ORNL-TM-5782, 1977). <https://doi.org/10.2172/7110792>
21. C.W. Lau, C. Demazière, H. Nylén et al., Improvement of LWR thermal margins by introducing thorium. *Prog. Nucl. Energy* **61**, 48 (2012). <https://doi.org/10.1016/j.pnucene.2012.07.004>
22. R.L. Murray, K.E. Holbert, Neutron chain reactions—nuclear energy. *Nucl. Energy* **16**, 259 (2015). <https://doi.org/10.1016/B978-0-12-416654-7.00016-2>. (Seventh Edition—Chapter 16)
23. J.J. Duderstadt, L.J. Hamilton, *Nuclear Reactor Analysis*, 1st edn. (Wiley, Berlin, 1976). <https://doi.org/10.1109/TNS.1977.4329141>
24. V. Barkauskas, R. Plukienė, A. Plukis, Actinide-only and full burn-up credit in criticality assessment of RBMK-1500 spent nuclear fuel storage cask using axial burn-up profile. *Nucl. Eng. Des.* **307**, 197 (2016). <https://doi.org/10.1016/j.nucengdes.2016.07.012>
25. *Reactivity Effects Due to Temperature Changes* (Nuclear Training Centre, Nuclear Theory, Course 427.00-12, OPG, 1990)